Rarefaction and Thermal Creep Effects in Square Cross-section Microchannels

Sridhar PALLE [1], Shahrouz ALIABADI [1*]

* Corresponding author: Tel.: ++1-601-979-1821; Fax: ++1-601-979-1831; Email: saliabadi@jsums.edu
1: Northrop Grumman Center for High Performance Computing, Jackson State University, MS e-Center,
1230 Raymond Rd, Jackson, MS, 39204, USA

Abstract Fluid flow and heat transfer in MEMS systems are numerically investigated in this study for potential rarefaction and thermal creep effects using our recently developed implicit, incompressible, hybrid (finite volume/finite element) flow solver. Rarefied flows characterized by the Knudsen number in the range of $0 \leq Kn \leq 0.1$ are analyzed in detail for thermal creep effects in square cross-section microchannels with constant wall temperature boundary condition. Axial conduction becomes important for very low Reynolds number flows thereby enhancing the thermal creep effect. Three dimensional numerical simulations are conducted for simultaneously developing flows at very low Reynolds numbers in the range of $0.2 \leq Re \leq 5$. Extended inlet boundary conditions are used to avoid entrance region singularity and also to account for axial heat conduction near the entrance. Friction coefficients are reduced with rarefaction in the slip flow regime. The reduction in friction coefficients was more pronounced due to thermal creep in the entrance region. Effects of rarefaction and thermal creep on heat transfer are studied for different gas-wall surface combinations as defined by the choice of momentum and thermal accommodation coefficients. It was found that heat transfer can increase or decrease with rarefaction. For very small values of gas-wall surface interaction parameter (β), it was observed that velocity slip dominates the temperature jump and heat transfer is enhanced with rarefaction. The opposite effect is observed for higher values of β. Nusselt number values increased slightly with thermal creep as Reynolds number was decreased.

Keywords: Thermal creep, micro-channel, Poiseuille number, Nusselt number, rarefaction

1. Introduction

Micro-fluidics has generated significant research interest in the last two decades. The rapid progress in micro fabrication technology has enabled this fairly new realm of engineering and technology to find many novel and diverse MEMS based applications; micro thermal cooling systems, micro sensors, accelerometers, micro-scale flows in medical devices, airways in human respiratory systems and other biological flows, and microporous media flows. Even though the technology is widespread and there have been many studies in the past, the fundamental understanding of flow physics involved in these devices is still very limited. The main challenges in studying the flows in these MEMS systems are the extremely small dimensions, which become comparable to the mean free path of the gas flowing through the system. The very small dimensions pose a challenge not only for experimental but also for theoretical studies.

When channel dimensions become comparable to molecular mean free path of the gas, the conventional continuum flow physics breaks down and the rarefied gas has to be modeled through different non-continuum models. For dilute gaseous flows, Knudsen number (Kn) (defined as the ratio of the molecular mean free path (λ) to the characteristic length (L) of flow device) classifies the deviation from continuum. Continuum approximation is valid for flows with very small Knudsen numbers ($Kn \leq 10^{-3}$) whereas for very large Knudsen numbers ($Kn \geq 10$) continuum assumption completely breaks down and fluid flows in this regime are treated as free molecular flows. Rarefied gases typically encountered in MEMS systems are neither completely in continuum nor in free molecular regime. Instead such flows are classified as slip flows ($10^{-3} \leq Kn \leq 10^{-1}$) and are the subject matter of present study.

Apart from the non-continuum effects, very small dimensions also present

instrumentation difficulties with experimental uncertainties and validating the numerical models becomes even bigger challenge. Nevertheless, in the past, several studies (Pfahler et al., 1991; Tison, 1993; Liu et al., 1995; Arkilic et al., 1995; Harley et al., 1995; Ebert and Sparrow, 1965; Wu and Little, 1983; Yu and Ameel, 2001; Morini et al., 2004) both experimental and theoretical have addressed the fluid flows in MEMS systems and have provided valuable insight into some key unconventional flow physics.

Numerical studies (Renksizbulut et al., 2006; Van Rij et al., 2007 and 2009; Hettiarachchi et al., 2008; Darabandi et al., 2009, Qazi Zade et al., 2010; Palle and Aliabadi, 2011) addressing the fluid flow and heat transfer in MEMS systems in the slip flow regime are limited. Review papers of Gad-el-Hak (1999) and Colin (2010) have much more detailed list of literature dealing with fluid mechanics and heat transfer in micro devices. The numerical treatment of flows in the slip regime typically involves the velocity and temperature jump modification for the boundary conditions in the Navier-stokes equations. Analytical and numerical studies confirm the necessity of slip velocity boundary modification with local shear using Maxwell's relation (Maxwell, 1879). However, most of the theoretical studies neglected the tangential temperature gradient contribution to slip velocity also called thermal creep phenomena. The assumption of negligible thermal creep is quite true for isothermal wall flows. However, in many practical MEMS based systems creeping flows (Re <<1), are often encountered making axial conduction very important especially in the entrance region of the flow channels. Temperature jump associated with rarefaction induces axial temperature gradients in the gas layer near the microchannel wall increasing the importance of thermal creep. Very few studies have addressed the effects of thermal creep in rarefied gaseous flows in the slip flow regime.

van Rij et al. (2007) recently studied gaseous creep flow in two-dimensional isoflux microchannels and observed that creep velocity effects are significant within the slip flow regime. They later extended their analysis to three-dimensional square cross-section micro channels to study the effects of viscous dissipation and rarefaction on heat transfer (van Rij et al., 2009). Méolans and Graur (2008) analytically studied thermal creep in parallel plate channels with constant temperature gradient along the channel walls. They have observed that curvature of the transverse velocity profiles changes after a transition point along the channel and becomes similar to isothermal profiles. Niazmand et al. (2009) studied thermal creep effects in isothermal wall channels with an extended adiabatic section assuming unity Prandtl numbers and unity momentum and thermal accommodation coefficients by control volume method. They found that thermal creep effects are significant in the entrance region for very low Reynolds number flows. Majority of the previous numerical studies are based on unity assumptions for accommodation coefficients which in principle depend on the choice of gas-wall surface interactions and can vary over a wide range from 0 to 1 (Eckert, 1972). Significant uncertainty exists in the literature regarding the accommodation coefficients which depend on the properties of gas, channel surface, and gas-wall surface interactions. Sharipov (2011) recently published a critical review on slip velocity and temperature jump coefficients and suggested improved expressions for accommodation coefficients.

In the present work, we have extended our recently developed hybrid Finite element/volume matrix-free flow solver for studying thermal creep effects in rarefied gaseous flows in the slip flow regime ($10^{-3} \leq Kn \leq 10^{-1}$) in square cross-section microchannels with isothermal walls. Very low Reynolds numbers in the range of ($0.2 \leq Re \leq 5$) are considered for analyzing the thermal creep phenomena in detail in simultaneously developing flows. Extended boundary conditions are employed to avoid entrance region singularity and also to properly account for axial heat conduction. Using three-dimensional numerical

simulations, fluid flow and heat transfer is thoroughly analyzed for any potential rarefaction and thermal creep effects for different values of gas-wall surface interaction parameter (β) which specifies the relative influence of velocity slip and temperature jump.

2. Problem Statement

Three dimensional numerical simulations have been conducted for square cross-section microchannels. Fig.1 shows the schematic of the microchannel. Due to the symmetry, only a quarter of the channel is modeled and the flow is considered along the length of the channel in the x-direction. Fluid flow and heat transfer in the microchannels is studied based on the assumptions of laminar, incompressible flow with negligible viscous dissipation. Governing equations based on the above assumptions are as follows:

$$\nabla.\mathbf{u}=0 \qquad (1)$$

$$\rho\left[\frac{\partial \mathbf{u}}{\partial t}+\mathbf{u}.\nabla \mathbf{u}\right]=-\nabla p+\mu\nabla^2\mathbf{u} \qquad (2)$$

$$\rho C_p\left[\frac{\partial T}{\partial t}+\mathbf{u}.\nabla T\right]=k\nabla^2 T \qquad (3)$$

The governing equations are non-dimensionalized using the following dimensionless parameters: hydraulic diameter (D_h) for the length scale, $\mathbf{u}^* = \mathbf{u}/U$, $p^* = p/\rho U^2$, $T^* = (T-T_i)/(T_w-T_i)$, where $\mathbf{u}$ is the velocity vector, ρ is the density, C_p is the specific heat at constant pressure, k is the thermal conductivity, μ is the dynamic viscosity, p is the pressure, T is the temperature, U is the inlet velocity and T_i is the inlet temperature of the fluid respectively. T_w is the constant wall temperature. Extended inlet boundary conditions are used where a fictitious inlet far upstream from the real inlet is defined where uniform velocity and temperature profiles are assigned instead of the real inlet. The walls of the extended channel are kept at symmetry boundary conditions. At the channel exit, zero axial gradients for velocity and temperature are applied and channel length is chosen such that hydrodynamically and thermally fully developed conditions are reached at the exit. The fluid flows at the boundary satisfying velocity slip and temperature jump. In the continuum flow regime, fluid is typically assumed to satisfy no-slip and no-temperature jump boundary conditions. However for MEMS, fluid flow adjacent to the wall is not in thermodynamic equilibrium and in the slip flow regime it has to satisfy the velocity and temperature jump boundary conditions. Maxwell (1879) and Smoluchowski (1898) derived the corresponding tangential velocity slip and temperature jump boundary conditions and in dimensionless form are as follows:

$$u_{gas}^*-u_w^* = \frac{2-\sigma_v}{\sigma_v}Kn\left(\frac{\partial u^*}{\partial n^*}\right)_w + Tcreep \qquad (4)$$

$$Tcreep=\left[\frac{3}{2\pi}\frac{(\gamma-1)}{\gamma}\frac{Kn^2Re}{Ec}\left(\frac{\partial T^*}{\partial x^*}\right)_w\right] \qquad (5)$$

$$T_{gas}^* - T_{wall}^* = \frac{2-\sigma_T}{\sigma_T}\left[\frac{2\gamma}{\gamma+1}\right]\frac{Kn}{Pr}\left(\frac{dT^*}{dn^*}\right)_w \qquad (6)$$

where *Tcreep* is thermal creep, γ is the specific heat ratio, Kn is the Knudsen number defined as the ratio of molecular mean free path to hydraulic diameter ($Kn = \lambda/D_h$), Re is the Reynolds number, Pr is the Prandtl number, and Ec is the Eckert number. In Eq. (4) slip velocity at the wall is related to local shear and the tangential temperature gradient in the fluid along the wall. Slip velocity contribution due to tangential temperature gradient is called thermal creep. In the definition of thermal creep, Eckert number is not a constant and is defined as follows:

$$Ec=\frac{U_i^2}{c_p(T_w-T_i)} \qquad (7)$$

The Knudsen number and Reynolds number are related through Mach number (Gad-el-Hak, 1999; Shokouhmand et al., 2011) as follows:

$$Kn=\sqrt{\frac{\pi\gamma}{2}}\frac{Ma}{Re} \qquad (8)$$

$$Ma=\frac{U_i}{\sqrt{\gamma RT_i}} \qquad (9)$$

Manipulating Eqs. (7) to (9), Eckert number can be defined in terms of Reynolds number, Knudsen number, inlet, and wall temperatures

and specific heat ratio as follows:

$$Ec = \frac{2}{\pi} \frac{T_i}{(T_w - T_i)} \frac{\gamma - 1}{\gamma} Kn^2 Re^2 \qquad (10)$$

Temperature jump modification in Eq. (6) relates the fluid temperature near the wall to normal temperature gradient at the wall. σ_v and σ_T are the tangential momentum and thermal accommodation coefficients respectively and are properties of gas-wall surface interaction and are dependent on the composition, temperature, velocity of gas on the surface, and also on the wall surface temperature, chemical state, and roughness. σ_v in principle can vary from 0 to 1 depending on specular to diffuse reflection of gas molecules from the surface, whereas σ_T can range from 0.01 to 1 (Eckert, 1972; Yu and Ameel, 2001). Sharipov (2011) recently published a critical review of slip velocity and temperature jump coefficients and suggested improved expressions for velocity and temperature jump coefficients. Based on experimental observations for many engineering applications where wall surfaces are not perfectly smooth, σ_v values are treated as being near unity. Recent experimental studies by Rader et al., (2005) listed σ_T values for nitrogen, argon, and helium gases over stainless steel surfaces. Values as low as 0.36 have been observed in their studies for helium. An extensive review on thermal accommodation coefficients has been provided by Saxena and Joshi (1981) and values as low as 0.07 have been reported. Since the values of accommodation coefficients depend on gas-wall surface combinations, three other parameters are defined as follows (Yu and Ameel, 2001; van Rij et al., 2009).

$$\beta_v = \frac{2 - \sigma_v}{\sigma_v} \qquad (11)$$

$$\beta_t = \left(\frac{2 - \sigma_T}{\sigma_T}\right)\left(\frac{2\gamma}{\gamma + 1}\right)\frac{1}{Pr} \qquad (12)$$

$$\beta = \frac{\beta_t}{\beta_v} \qquad (13)$$

$\beta_v Kn$ defines the slip contribution and $\beta_t Kn$ defines the temperature jump contribution for any gas-wall surface combination. β specifies relative influence of temperature jump coefficient over velocity slip coefficient. β_t

values can become quite large since σ_T values as low as 0.07 have been observed for very smooth surfaces. For sample systems of nitrogen, helium, and argon over stainless steel surface as listed in the recent work of Rader et al., (2005) β values fall in the range of 1 to 10. Sharipov (2011) has also observed that for light gases temperature jump coefficients can increase significantly. For most of the engineering applications, β or β_t could be greater than unity implying significant temperature jump with rarefaction. $\beta < 1$ values are possible when velocity slip is dominant than temperature jump, and $\beta = 0$ is the limiting case for such flows and also when velocity slip is considered but not temperature jump. In the present study our main goal was to evaluate the relative effects of velocity slip and temperature jump on fluid flow and heat transfer respectively. Therefore rather than studying a particular gas-wall surface combination (which would require accurate values of accommodation coefficients), we have analyzed the rarefaction and thermal creep effects in terms of different lower ($\beta<1$, velocity slip is dominant) and higher ($\beta>1$, temperature jump is dominant) values of gas-wall surface interaction parameter.

3. Numerical Method

The incompressible governing equations are solved using our recently developed implicit hybrid (finite volume/finite element) flow solver which is based on a pressure correction or projection method. We use the cell-centered finite volume method (FV) to solve the momentum equation for the intermediate velocity and the node-based Galerkin finite element method (FE) to solve the Poisson equation for the pressure correction. Note that in our implementation, the pressure does not directly enter the momentum equation. Instead, an auxiliary variable closely related to the pressure takes the place of pressure in the momentum equations. The auxiliary variable updates the pressure and velocity fields. Numerical results have shown that the current hybrid implementation is superconvergent in terms of the spatial convergence rates for both

velocity and pressure. The complete details of the development and implementation of our matrix free, implicit, hybrid finite volume/element flow solver are presented in the earlier work of Aliabadi et.al. (2007).

Grid independence was achieved for a mesh beyond 51 x 51 x 241 in the y, z, and x directions respectively. Also grid points were clustered near the channel entrance and walls due to presence of significant velocity and temperature gradients. Table 1 and Table 2 shows the grid independent Nusselt numbers compared with the work of van Rij et al. (2009). For $Kn > 0$, Nu values obtained from van Rij et al. (2009) are from their figures and therefore are approximate in nature. Nevertheless it can be seen that Nusselt numbers are in very good agreement. The complete validation of the extension of our hybrid FE/FV flow solver for MEMS flows with analytical and experimental data in the slip flow regime has been documented in detail in our earlier work (Palle and Aliabadi, 2011).
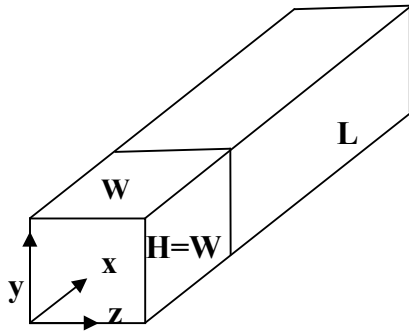
Fig. 1. Schematic of square cross-section microchannel

Table 1
Grid independence and comparison of fully developed Nusselt numbers, $Kn = 0$, $Re = 0.715$, $Pr = 0.7$ ($Pe = 0.5$)

Present Work		van Rij et al. (2009)	
Grid	Nu	Grid	Nu
21 x 21 x 241	3.48	10 x 10 x 120	3.404
31 x 31 x 241	3.43	20 x 20 x 240	3.372
51 x 51 x 241	3.35	40 x 40 x 480	3.364

Table 2
Fully developed Nusselt numbers for different Kn values at $Re = 0.715$, $Pr = 0.7$ ($Pe = 0.5$)

Kn	0.0	0.04	0.08	0.12
Present results	3.34	3.11	2.69	2.29
van Rij et al. (2009)	3.37	3.1	2.65	2.31

4. Results

Three-dimensional numerical simulations are conducted with square cross-section microchannels for evaluating the rarefaction and thermal creep effects. Rarefied gases with Knudsen numbers in the range of $10^{-3} \leq Kn \leq 10^{-1}$ are considered and flow Reynolds numbers are varied from 0.2 to 5. The gas enters the microchannel at $T_i = 293K$, and the microchannel wall temperature is kept at $T_w = 373K$. The results that are presented below are for unity Prandtl number, $\gamma = 1.4$, and accommodation coefficients are varied so that results are analyzed for different gas-wall surface interaction parameter values in the range of $0.1 \leq \beta \leq 2$.

4.1 Fluid Velocity
To gain a clear understanding of the influence of thermal creep on fluid flow, velocity profiles are plotted in Fig. 2 for $Re = 0.2$.
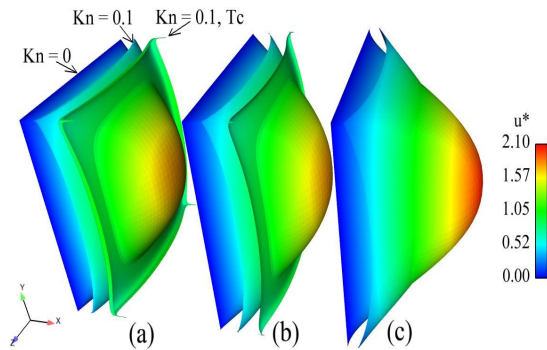
Fig. 2. Velocity profiles at entrance (a) $x^*/Re = 0.005$, (b) $x^*/Re = 0.05$ and fully developed (c) $x^*/Re = 5$ for $Re = 0.2$, $\beta = 1.16$.

Velocity profiles are shown in three different axial locations and profiles with no-slip, slip, and slip with thermal creep for $Kn = 0.1$ are superimposed on each other. With this kind of representation thermal creep influence is more

obvious. Rarefaction flattens the velocity profiles compared to no-slip. Thermal creep increases the slip velocity at the boundary, but only in the entrance region where tangential temperature gradients become important due to the temperature jump associated with rarefaction. It can be observed that due to thermal creep in the entrance boundary slip velocities are higher and gradually reduce back to the no-thermal creep case in the fully developed region where both velocity profiles are identical. With thermal creep velocity over-shoots or discontinuities are also observed at the four corners in the very entrance region. This is because a normal doesn't exist for sharp corners and also because tangential temperature gradients are maximal at the corners. Effects of thermal creep for different Reynolds numbers are shown in Fig. 3 for $Kn = 0.1$ and $\beta = 1.16$ where peripherally averaged slip velocity is plotted along the channel length. Axial conduction increases as Reynolds number decreases and hence the tangential temperature gradients increase in the entrance region resulting in higher slip velocity at the wall. It can also be seen that thermal creep doesn't influence the fully developed region.
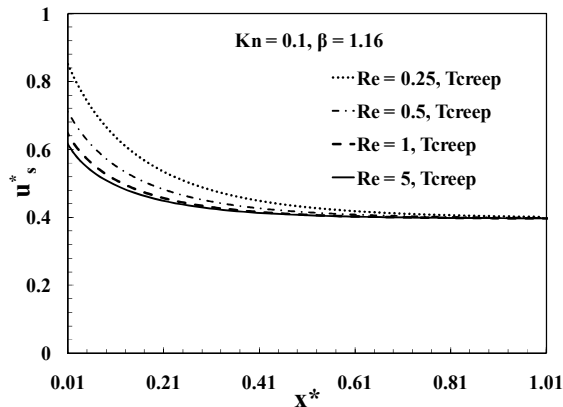
Fig. 3. Slip velocity at different *Re* values.

Influence of rarefaction, thermal creep, and β on the slip velocity is shown in Fig. 4 for $Re = 1$. It can be observed that slip velocities increase with increasing rarefaction due to the increased velocity jump associated with *Kn*. Thermal creep further increases the slip velocity in the entrance due to the tangential

temperature gradient contribution which arises due to temperature jump with rarefaction.
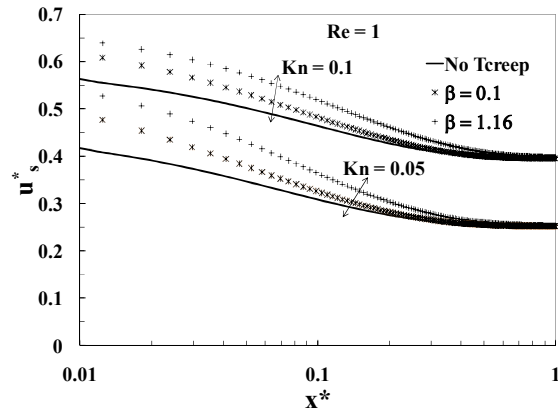
Fig. 4. Slip velocity with and without thermal creep at $Re = 1$, for different β and Kn.

As the temperature jump is reduced relative to velocity jump as shown by the smaller β values, slip velocity approaches the no-thermal creep values in the entrance.

4.2 Friction Factors

The effect of increased slip at the boundary with thermal creep has a more profound effect on Fanning friction factors or Poiseuille numbers plotted in Fig. 5. As the Reynolds number decreases, slip velocity increases and the velocity profiles becomes much flatter at the entrance compared to the case when thermal creep is not included. This causes normal component of velocity gradients to reduce much sharply at lower *Re* values, resulting in significant drop in friction coefficients at the entrance. Infact, as was shown in Fig. 2, for $Re = 0.2$, curvature of velocity profile at the boundary reverses compared to the inner core region. As the Reynolds number increases, thermal creep effect begins to disappear as can be seen from the friction coefficient for $Re = 5$.

The effect of rarefaction, thermal creep, and β on friction coefficients is shown in Fig. 6. Compared to no-slip case, friction coefficients are reduced significantly with rarefaction due to slip velocity and reduced velocity gradients. The reduction is even more pronounced with thermal creep due to much

higher slip velocities and more flatter velocity profiles.
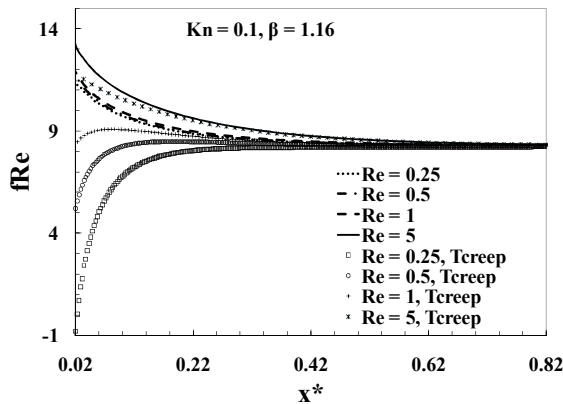
Fig. 5. Poiseuille numbers at different *Re* values.

At a particular value of *Kn*, as *β* is reduced temperature jump is reduced relative to velocity jump and friction coefficients with thermal creep approach the no-thermal creep values.
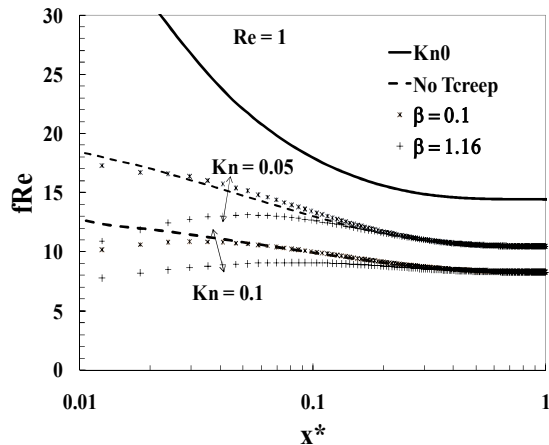
Fig. 6. Poiseuille numbers with and without thermal creep at *Re* = 1, for different *β* and *Kn* values.

4.3 Nusselt Numbers

To analyze the influence of non-unity accommodation coefficients, peripherally averaged Nusselt numbers are plotted for different values of *β* and *Kn* = 0.1 without thermal creep in Fig. 7. It can be observed that with an increase in *β*, temperature jump increases with a tendency to reduce heat transfer because of smaller temperature gradients at the boundary wall. On the

contrary, as *β* is reduced, temperature jump effect decreases and velocity slip becomes dominant which has a tendency to increase the heat transfer. Therefore depending on which factor (velocity slip or temperature jump) is relatively dominant, heat transfer can increase or decrease with rarefaction. As can be observed from Fig. 7 for *β* = 0.1 Nusselt number values are higher with rarefaction for most of the channel length compared to the no-slip case, whereas for the same degree of rarefaction (*Kn* = 0.1), for *β* = 1.16 and *β* = 2 Nusselt numbers are lower suggesting a reduction in heat transfer. Thus it becomes clear as to the importance of accommodation coefficients in accurately evaluating the effects of rarefaction on heat transfer. It is the relative importance of velocity slip and temperature jump which in turn depends on the relative values for momentum and thermal accommodation coefficients which determines the influence of rarefaction on heat transfer.
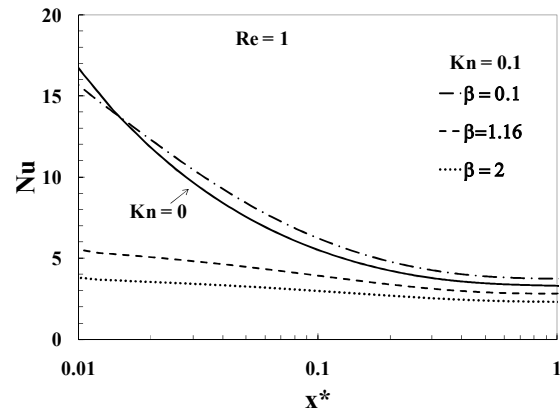
Fig. 7. Comparison of Nusselt numbers for *Kn* = 0.1 at different *β* values, with *Kn* = 0.

The influence of thermal creep on Nusselt number at different Reynolds numbers is shown in Fig. 8 for *Kn* = 0.1 and *β* = 1.16. As the Reynolds number decreases which increases the axial conduction, Nusselt number increases modestly throughout the channel length. Influence of thermal creep for different *β* and *Kn* values is also plotted for *Re* = 1 in Fig. 9. It can be seen that compared to the no-slip case heat transfer is reduced with rarefaction for *β* = 1.16 and enhanced at *β* = 0.1. However, thermal creep doesn't seem to have much influence on the heat transfer.
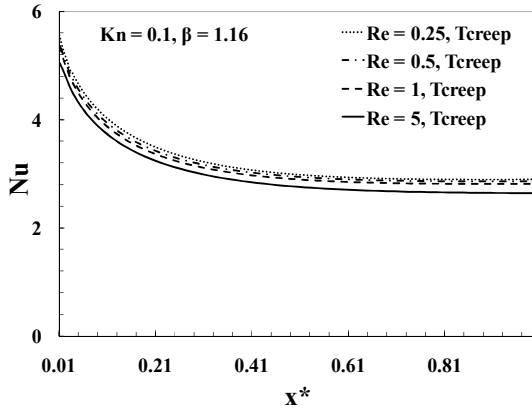
Fig. 8. Nusselt numbers at different *Re* values.
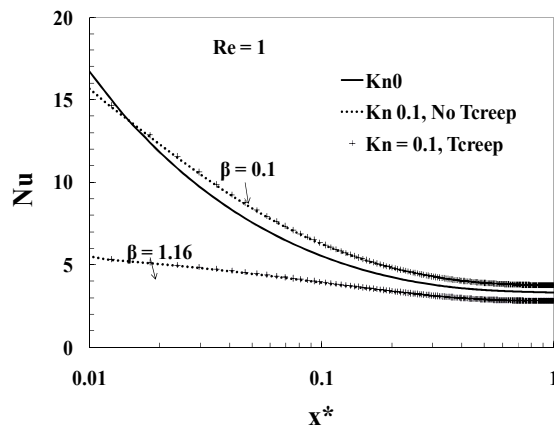
Fig. 9. Nusselt numbers with and without thermal creep at different *Kn* and *β* values.

This could be explained based on the fact that for such low Reynolds number flows, axial conduction and hence the increase in slip velocity due to thermal creep is only in the very entrance region for the current constant wall temperature study. Increase in the slip-velocity due to thermal creep at the entrance may not be dominant enough relative to the temperature jump due to rarefaction to cause any appreciable increase in heat transfer. Therefore even though slip velocity is higher with thermal creep, it may not be strong enough to counter the temperature jump effect.

5. Conclusions

Rarefaction and thermal creep effects are evaluated in the square cross-section microchannels in the slip flow regime for low Reynolds number flows at different values of

gas-wall surface interaction parameter *β*. Rarefaction increases the slip velocity with flatter velocity profiles compared to the no-slip case and reduces the velocity gradients at the boundary wall and decreases the friction coefficients. Rarefaction also causes temperature jump at the boundary which results in tangential temperature gradients in the gas layer near the wall in the entrance region. Since axial conduction increases as the Reynolds number is decreased tangential temperature gradients at the entrance increase resulting in higher slip velocities at the wall boundary due to thermal creep. The increase in the slip velocity is accompanied by flatter velocity profiles and much smaller velocity gradients. Therefore friction coefficients at the entrance are much smaller compared to the case when thermal creep is not considered.

Rarefaction effects the heat transfer depending on the relative strength of velocity slip compared to the temperature jump. For very small *β* values heat transfer is enhanced compared to the no-slip case, whereas heat transfer is reduced for higher *β* values. For most of the engineering applications, with $Pr \sim 0.7$, $\gamma \sim 1.4$, *β* could be greater than unity with rarefaction reducing heat transfer. $\beta = 0.1$ is more or less a limiting case, even though $\beta < 1$ values are possible. Increased slip velocities due to thermal creep modestly increases the heat transfer as Reynolds number is decreased. Slip velocity due to thermal creep for higher *Re* values is not dominant enough compared to the temperature jump to cause any significant effect on heat transfer.

References

Aliabadi, S., and Tu, S., 2007. Hybrid finite element / finite volume flow solver for flow and transport problems, 14th International Conference on Finite Elements in Flow Problems, Santa Fe, New Mexico, March 26-28, 2007.

Arkilic, E.B., Schmidt, M.A., Breuer, K.S., 1995. Slip flow in mirochannels. Rarefied Gas Dynamics 19, J. Harvey and G. Lord, eds., Oxford University Press, Oxford, UK.

Colin, S., Gas microflows in the slip flow regime: a review on heat transfer, in Proceedings of the 3rd Joint US-European Fluids Engineering Summer Meeting and 8th International Conference on

Nanochannels, Microchannels and Minichannels (FEDSM-ICNMM2010), Montréal, Canada. ASME, pp. FEDSM-ICNMM2010-30167:1-14, 2010.

Darabandi, M., and Vakilipour, M., 2009. Solution of thermally developing zone in short micro-nanoscale channels. Journal of Heat Transfer, 131, 044501, 1-5.

Ebert, W.A., and Sparrow, E.M., 1965. Slip flow in rectangular and annular ducts. J. Basic. Eng., Trans, ASME, 1018-1024.

Eckert, E.G.R., 1972. Analysis of Heat and Mass Transfer, McGraw-Hill, NY, 467-486.

Gad-el-Hak, M., 1999. The fluid mechanics of microdevices-the Freeman scholar lecture. Journal of Fluids Engineering, 121, 5-31.

Harley, J.C., Huang, Y., Bau, H.H., Zameel, J.N., 1995. Gas flow in Micro-channels. Journal of Fluid Mechanics, 284, 257-274.

Hettiarachchi, H.D.M., Golubovic, M., Worek, W.M., Minkowycz, W.J., 2008. Three-dimensional laminar slip flow and heat transfer in a rectangular microchannel with constant wall temperature. Int. J. Heat Mass Transfer, 51, 5088-5096.

Liu, J., Tai, Y.C., Pong, K., Ho, C.M., 1995. MEMS for pressure distribution studies of gaseous flows in microchannels. Proceedings, IEEE Micro Electro Mechanical Systems, 209-215.

Maxwell, J.C., 1879. On stresses in rarefied gases arising from inequalities of temperature. Philosophical Transactions of the Royal Society, Part1, 170, 231-256.

Méolans, J.G., and Graur, I.A., 2008. Continuum analytical modeling of thermal creep. European Journal of Mechanics-B/Fluids, 27(6), 785-809.

Morini, G.L., Spiga, M., Tartarini, P., 2004. The rarefaction effect on the friction factor of gas flow in microchannels. Superlattices and Microstructures, 35, 587-599.

Niazmand, H., Jaghargh, A.A., Renksizbulut, M., 2009. Thermal creep effects in isothermal wall microchannels. The 20th international Symposium on Transport Phenomena, July 7-10, Victoria BC, Canada.

Palle, S., and Aliabadi, S., 2011. Slip flow and heat transfer in rectangular microchannels using Hybrid FE/FV method. International Journal of Numerical Methods in Engineering, Published online in Wiley Online Library (wileyonlinelibrary.com). DOI: 10.1002/nme.3231

Pfahler, J., Harley, J., Bau, H., Zemel, J.N., 1991. Gas and liquid flow in small channels. Symposium on Michromechanical Sensors, Actuators, and Systems, ASME DSC-32, 49-60.

Qazi Zade, A., Renksizbulut, M., and Friedman, J., 2010.Variable property effects in simultaneously developing gaseous slip-flow in rectangular microchannels with prescribed wall heat flux, in Proceedings of the 3rd Joint US-European Fluids Engineering Summer Meeting and 8th International Conference on Nanochannels,Microchannels and Minichannels (FEDSM-ICNMM2010), Montréal, Canada. ASME, pp. FEDSM-ICNMM2010-30587:1-8.

Rader, D.J., Trott, W.M., Torczynski, J.R., Castaneda, J.N., Gallis, M.A., Gocherg, L.A., 2005. Measurements of thermal accommodation coefficients. *SAND 2005-6084;* Sandia National Laboratories, USA.

Renksizbulut, M., Niazmand, H., Tercan, G., 2006. Slip-flow and heat transfer in rectangular microchannels with constant wall temperature. International Journal of Thermal Sciences, 45, 870-881.

Saxena, S.C., Joshi, R.K., 1981. Thermal accommodation and adsorption coefficients of gases. McGraw Hill, New York.

Sharipov, F., 2011. Data on the velocity slip and temperature jump on a gas-solid interface, *Journal of Physical and Chemical Reference Data*, vol. 40, n° 2, pp. 023101:1-28.

Shokouhmand, H., Bigham, Sajjad., Isfahani, R.N., 2011. Effects of Knudsen number and geometry on gaseous flow and heat transfer in a constricted microchannel. Heat Mass Transfer, 47, 119-130.

Smoluchowski, von M., 1898. Über wärmeleitung in verdünnten gasen, Ann. Phys. Chem, 64, 101–130.

Tison, S.A., 1993. Experimental data and theoretical modeling of gas flows through metal capillary leaks. Vacuum, 44, 275-292.

Van Rij, J.V., Harman, T., Ameel, T., 2007. The effect of creep flow on two-dimensional isoflux microchannels. International Journal of Thermal Sciences, 46, 1095-1103.

Van Rij, J., Ameel, T., and Harman, T., 2009. The effect of viscous dissipation and rarefaction on rectangular microchannel convective heat transfer, International Journal of Thermal Sciences, vol. 48, n° 2, pp. 271-281.

Wu, P., and Little, W.A., 1983. Measurement of friction factors for the flow of gases in very fine channels used for microminiature joule-thomson refrigerators. Cryogenics, 23, 273-277.

Yu, S., and Ameel, T.A., 2001. Slip-flow heat transfer in rectangular microchannels. Int. J. Heat Mass Transfer, 44, 4225-4234.